JOURNAL OF COMPUTATIONAL PHYSICS 9, 339–364 (1972)

A Numerical Method for Three-Dimensional Viscous Flow: Application to The Hypersonic Leading Edge*

STANLEY G. RUBIN† AND TONY C. LIN‡

Polytechnic Institute of Brooklyn,
Preston R. Bassett Research Laboratory,
Farmingdale, New York

Received May 4, 1971

A predictor-corrector multiple iteration method is formulated to treat three-dimensional viscous flow problems. Specific application is made to the viscous interaction near a hypersonic leading edge. The effects of iteration on accuracy, stability and consistency of the finite-difference solutions is evaluated for both leading-edge calculations and a model Burgers' equation. For a right-angle corner geometry comparisons are made with explicit finite-difference solutions and some recent experimental data.

I. INTRODUCTION

In a series of recent papers [1–7] it has been shown that at moderate angles of attack, the continuum flow over a slender body having a sharp leading edge can be described with a boundary-layer like system of equations. This model represents a uniformly valid approximation to the Navier–Stokes equations and applies throughout the inner viscous and shock layers, as well as the structure of the outer shock wave, Fig. 1. This unified approach to viscous–inviscid interactions has been developed to examine the flow in the leading-edge region of both two-dimensional [1–5] and more complex three-dimensional geometries [4–7]. Solutions of the governing equations have been obtained by numerical methods.

At first, numerical investigations of the hypersonic leading-edge equations were

* This research sponsored by the Air Force Office of Scientific Research, Office of Aerospace Research, USAF, under Grant No. AFOSR 70-1843 and Modification No. AFOSR 70-1843A. The United States Government is authorized to reproduce and distribute reprints for Governmental purposes notwithstanding any copyright notation hereon.

† Associate Professor of Aerospace Engineering.

‡ This work is based in part upon a dissertation by the second author to the Polytechnic Institute of Brooklyn in partial fulfillment of the requirements for the degree of Doctor of Philosophy (Astronautics) June 1970. Post-Doctoral Fellow.

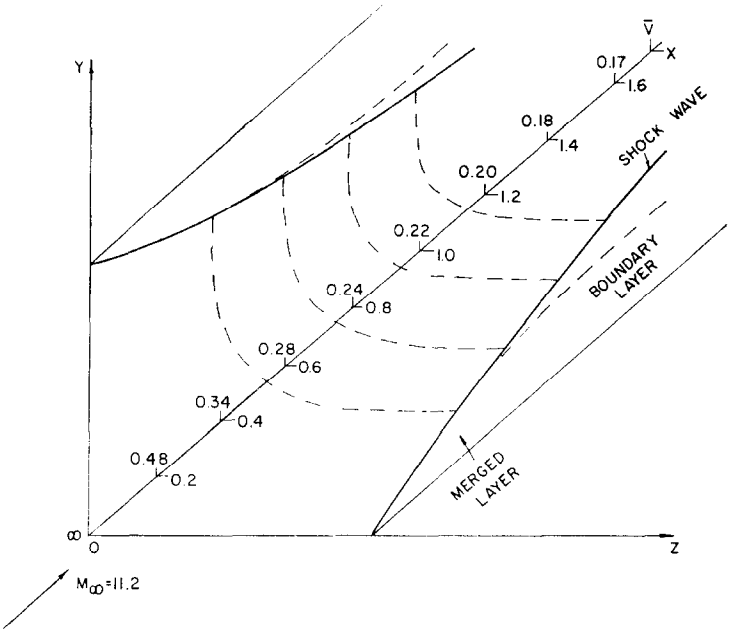

FIG. 1. Corner geometry: leading-edge region.

primarily concerned with the validity of the flow model and therefore, the ability to accurately describe the formation of constant-pressure boundary layers, outer shock structure, and measurable surface properties. Comparisons with all available experimental data have been very good, except in the shock structure for strong shock waves where the Navier–Stokes model is inadequate. Initial solutions were obtained with a simple explicit finite-difference scheme [1]. In order to progress further downstream of the leading edge, less time-consuming implicit methods were subsequently applied for two-dimensional geometries [2–4]. Detailed comparisons of various explicit and implicit finite-difference methods as applied to two-dimensional and axisymmetric leading-edge flows are given by Rubin and Lin [5].

For three-dimensional flows, the system of linearized algebraic finite-difference equations becomes undesirable, from the point of view of numerical analysis, with totally implicit methods. With k dependent variables and m, n grid points in the y, z directions, respectively, (see Fig. 2) kmn equations are generated. Typically, for leading-edge or time-dependent analyses, $k = 4$ and $m, n > 30$. Even with significantly larger marching steps than allowable with an explicit formulation, the inversion matrices become so large that calculation times may not be significantly decreased, a high degree of accuracy is not achievable, and computer storage becomes excessive.

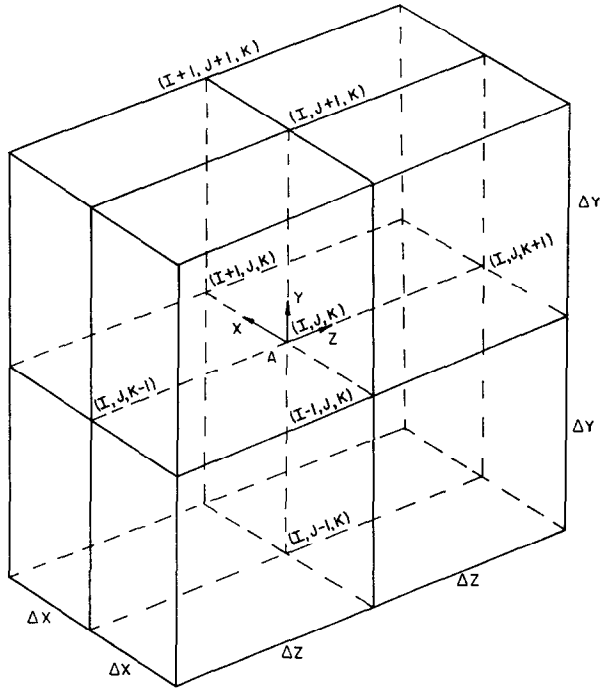

FIG. 2. Three-dimensional finite-difference grid.

The purpose of this paper is to describe a predictor-corrector, multiple iteration technique that has been developed for three-dimensional viscous flows, and in particular, for application near leading edges. Our objective is to minimize calculation times and yet retain a high degree of accuracy at each downstream location, or for unsteady flows in the transient motion. The method is applicable to three-dimensional boundary layers, three-dimensional boundary regions where diffusion is significant in two directions, and for two-dimensional unsteady solutions of the Navier–Stokes equations.

The finite-difference formulation represents a compromise between modified implicit approaches such as the alternating-direction scheme of Peaceman and Rachford [8] or the three-dimensional boundary layer method of Krause [9], and a modified explicit approach discussed by Evans et al. [10] and applied in time-dependent studies by Crocco [11] and Cheng [12].

The finite-difference formulation is presented in Section III where the use of iteration to treat the nonlinearities of the difference equations is discussed. Sections IV and V are concerned with the effect of iteration on the stability and consistency of the finite-difference scheme, respectively. The need for multiple

iteration in order to provide acceptable accuracy at each streamwise location, or in the transient, when larger step sizes are chosen, is described by a numerical experiment with the two-dimensional Burgers' equation.

In Section VI, the finite-difference method is applied to the three-dimensional leading-edge equations for the flow along a right-angle corner. Comparisons are made with explicit finite-difference solutions [6] obtained with step sizes two orders-of-magnitude smaller than those assumed here, and requiring computer times that are larger by more than one order-of-magnitude. Comparisons are also made with some leading-edge experimental data for the corner geometry.

II. Symbols

$A_{I+1,J,K}$	matrix
$B_i(J), C_i(J)$	column vectors
$\sqrt{c}$	Chapman–Rubesin constant
$c = v/u, d = w/u$	
I, J, K	finite-difference grid points in x, y, z directions, respectively
M_∞	Mach number
m	iteration number
l, n	indices in stability analysis
p	pressure
$\mathrm{Re} = uv^{-1}$ or v^{-1}	unit Reynolds number
$\mathrm{Re}_\infty = u_\infty x/v$	
$\mathrm{Re}_z = (\mathrm{Re})z, \mathrm{Re}_x = (\mathrm{Re})x$	
t	time
T	temperature
u, v, w	velocity components in x, y, z, direction, respectively
U_∞	free-stream velocity
$\bar{V}$	Rarefaction parameter $\bar{V} = M_\infty \sqrt{c}/\sqrt{\mathrm{Re}_\infty}$
α_n	consistency factor $\alpha_n = 1 - [\beta/(1+\beta)]^{n+1}$

$\beta_1\beta_2$	$\beta_1 = \mathrm{Re}^{-1}\,\Delta x/\Delta y^2$, $\beta_2 = \mathrm{Re}^{-1}\,\Delta x/\Delta z^2$
ξ	amplification factor
γ	constant
ϵ	either 0 or 1
κ_1	$c\Delta x/2\Delta y$, $\kappa_2 = d\Delta x/2\Delta z$
λ	$1.26\nu/T^{1/2}$
ν	kinematic viscosity
ρ	density
$\bar{\chi}$	interaction parameter
$\bar{\chi} = \sqrt{c}\,M_\infty^3/\sqrt{\mathrm{Re}_\infty}$	

III. Finite-Difference Method: Nonlinearity and Iteration

In Section VI numerical solutions for the three-dimensional flow near the leading edge of a right-angle corner are obtained with a predictor-corrector finite-difference formulation. In order to describe this multistep method and, in particular, the effect of iteration on nonlinearity, stability and consistency, numerical solutions of the leading-edge equations will be critically examined. Also, the following simplified model, representative of the system (13), will be analyzed:

$$u_x + cu_y + du_z = \mathrm{Re}^{-1}(u_{yy} + \epsilon u_{zz}). \tag{1}$$

For leading-edge or boundary-region analyses $\epsilon = 1$; for three-dimensional boundary-layer studies $\epsilon = 0$. For steady flow $c = v/u$, $d = w/u$, $\mathrm{Re} = u/\nu$; for unsteady two-dimensional Navier–Stokes considerations, $\epsilon = 1$, $(x, y, z) \to (t, y, x)$, $c = v$, $d = u$ and $\mathrm{Re} = \nu^{-1}$. u, v, w are the velocity components in the x, y, z directions, respectively. ν is the kinematic viscosity.

If y is chosen as the direction in which the gradients are a maximum, e.g., normal to the surface or boundary layer or shear layer, then z (in steady flow) or x (in unsteady flow) is termed the lateral direction. When $\epsilon = 0$, lateral diffusion is considered unimportant. For many flow configurations, this approximation may be a generally but not a locally valid approximation. Among these are the corner geometry discussed in Section VI and three-dimensional problems with cross-flow separation or with large local cross-flow gradients induced by geometry or boundary

conditions, e.g., large local transverse curvature or discontinuous lateral boundary values.

Our objectives in selecting a suitable finite-difference formulation are (1) to minimize computer running times by the elimination of viscous stability conditions as well as any stability limitation dependent on the normal (y) grid size; (2) to eliminate cross coupling of grid points, in the normal and lateral directions, in the finite-difference equations. In this way, the inversion matrices are reduced, computer times are decreased and computational accuracy is increased; (3) to allow for simple application to problems where symmetry or derivative boundary conditions play an essential role; (4) to maintain a minimum level of storage and still retain desired accuracy; (5) to make the computer code as simple as possible; and (6) to use iteration as a means of insuring acceptable accuracy of the nonlinear difference equations.

To accomplish these aims, a finite-difference scheme implicit in the normal or y-direction, with efficient use of iteration to minimize lateral grid size instability and insure second-order accuracy and consistency, is formulated. From a practical point of view, it was found by numerical experiment, that this method is superior to the implicit alternating-direction scheme of Peaceman and Rachford [8], when applied to the leading-edge equations [1]. This alternating-direction method cannot be applied to three-dimensional boundary layers, since diffusion appears in only one direction.

Nonlinear leading-edge calculations using the alternating-direction scheme, and without iteration, have been examined by the authors. These calculations are not unconditionally stable as the linear theory predicts. Relatively small streamwise increments are required in order to obtain stable solutions. These instabilities also appear in implicit two-dimensional calculations but are suppressed with iteration so that somewhat larger step sizes can be prescribed. The effect of iteration on two-dimensional, nonlinear instability is discussed in greater detail later in this section. The alternating-direction method is also less attractive than the predictor-corrector formulation for several other reasons. In view of the asymmetric treatment of derivatives, it is difficult to enforce symmetry conditions as required along a diagonal for the corner geometry; similar difficulties with lateral boundary conditions occur with other nonrectangular geometries, such as a cone at incidence. Furthermore, unilateral iteration in any one direction results in instability; the lateral grid spacings must remain equal throughout the calculation[1] and this numerical method appears to be extremely sensitive to the choice of initial conditions (see Nardo and Cresci [7]).

Consider a finite-difference grid as given in Fig. 2; the finite-difference formulas

[1] For the corner geometry a variable lateral grid is prescribed to reduce the computer storage and calculation time.

can be centered at $I+1$ (as with a "fully-implicit" method) or at $I+\frac{1}{2}$ (Crank–Nicolson).

For the $(I+\frac{1}{2})$ multistep formulation, the following finite-difference representations accurate to $O(\Delta x^2, \Delta y^2, \Delta z^2)$ are postulated:

$$u_y = (1/4\Delta y)[u_{I+1,J+1,K} - u_{I+1,J-1,K} + u_{I,J+1,K} - u_{I,J-1,K}], \tag{2a}$$

$$u_{yy} = (1/2\Delta y^2)[u_{I+1,J+1,K} + u_{I+1,J-1,K} - 2u_{I+1,J,K} + u_{I,J+1,K} + u_{I,J-1,K} - 2u_{I,J,K}], \tag{2b}$$

$$u^{m+1}_{I+1/2,J,K} = \tfrac{1}{2}[u^m_{I+1,J,K} + u_{I,J,K}], \tag{2c}$$

$$u_x = (1/\Delta x)[u_{I+1,J,K} - u_{I,J,K}], \tag{2d}$$

$$u^{m+1}_{zz} = (1/2\Delta z^2)[u^m_{I+1,J,K+1} + u^m_{I+1,J,K-1} - 2u^{m+1}_{I+1,J,K} + u_{I,J,K+1} + u_{I,J,K-1} - 2u_{I,J,K}], \tag{2e}$$

$$u^{m+1}_z = (1/4\Delta z)[u^m_{I+1,J,K+1} - u^m_{I+1,J,K-1} + u_{I,J,K+1} - u_{I,J,K-1}], \tag{2f}$$

$$(uv)_{I,J,K} = \tfrac{1}{2}[u^{m+1}v^m + u^m v^{m+1}]_{I,J,K}. \tag{2g}$$

Similar equations are obtained when the differences are centered at $I+1$; but if second-order accuracy is to be maintained, (2d) will include a $u_{I-1,J,K}$ term. The subscript m denotes the iteration number.

The finite-difference equations (2) are affected by iteration in two distinct ways; (i) linearization of nonlinear terms, viz. (2g), and (ii) the manner in which lateral derivatives are formulated, viz. (2e). For the first step of the iterative cycle, terms with superscript zero, e.g., $u^0_{I+1,J,K}$, are approximated by

(1) *linear replacement*: $$u^0_{I+1,J,K} = u_{I,J,K} + O(\Delta x), \tag{3a}$$

(2) *Taylor series to* $O(\Delta x^2)$: $$u^0_{I+1,J,K} = 2u_{I,J,K} - u_{I-1,J,K} + O(\Delta x^2). \tag{3b}$$

In this section only the effects of iteration on linearization are discussed. Two-dimensional implicit calculations are considered with formulas (2a) and (2b). The effect of iteration with the modified lateral difference formulas (2e) and (2f) is discussed in Section V.

With the linearization formulas (3a) or (3b) and the finite-difference relationships (2), or those centered at $I+1$, two planes I and $I+1$ remain in storage at all times. The $I-1$ value in (3b) is immediately replaced with the newly calculated $I+1$ result. With (3b), the finite-difference equations remain second-order accurate expressions of the differential equations. There is, however, a second-order error introduced in the relationship between the linearized and exact nonlinear finite-

TABLE I

Effect of Iteration (Linearized Implicit Calculations)[a]

No. of iteration	$\bar{V}$	u at Wall	v at $y = \Delta y$	T at Wall	$C_H/\bar{V}^{3/2}$	u_y at $y = \frac{1}{2}\Delta y$	u_y at $y = \Delta y$	$\bar{\rho}_{max}$	$\bar{\rho}_y$ at $y = \Delta y/2$	Δx
0		0.52414	−0.026589	5.06869	0.40901	0.707355	0.731523	1.71007	−1.11922	
1	0.38405	0.39119	−0.032464	5.60448	0.42916	1.422532	1.170671	1.74244	0.553450	0.005
2		0.39111	−0.032531	5.61008	0.42999	1.422916	1.170691	1.73798	0.546962	
3		0.39111	−0.032551	5.61006	0.42999	1.422932	1.170706	1.73798	0.546801	
0	unstable	—	—	—	—	—	—	—	—	
1		0.32490	−0.016495	5.96235	0.46463	0.946983	0.914235	2.09568	0.218200	
2	0.29616	0.32469	−0.016438	5.97191	0.46657	0.947611	0.914756	2.07967	0.180787	0.01
3		0.32467	−0.016426	5.97200	0.46659	0.947630	0.914781	2.07920	0.178512	
0	unstable	—	—	—	—	—	—	—	—	
1		0.25140	−0.006683	6.23582	0.49892	0.683230	0.669882	2.63452	−0.12484	
2	0.22000	0.25116	−0.006881	6.24867	0.50279	0.686230	0.670771	2.56918	−0.129675	0.02
3		0.25115	−0.006889	6.24880	0.50286	0.686230	0.670771	2.56759	−0.129676	
0	unstable	—	—	—	—	—	—	—	—	
1		0.21104	−0.003895	6.31431	0.51765	0.554661	0.545053	2.89689	−0.146683	
2	0.18292	0.21056	−0.003841	6.33024	0.52341	0.555737	0.546043	2.78782	−0.151205	0.02
3		0.21055	−0.003835	6.33038	0.52347	0.555760	0.546065	2.78602	−0.151265	

[a] Axisymmetric cone: $M_\infty = 7.95$, $\Delta y = 0.08$.

difference equations. For this reason, derivatives evaluated from the solutions obtained at station $I + 1$ may incur a somewhat larger error; e.g., if the error created by the linearization in u is $O(\Delta x^2)$, u_y may be in error by $O(\Delta x^2/\Delta y)$. If Δx and Δy are poorly chosen, the error due to linearization may be singificant.

The system of equations governing the flow near a leading-edge in two or three dimensions is nonlinear and includes products of derivatives [1, 4, 5]. This means that certain derivative functions must also be linearized. Since the errors in these derivative expansions may be substantial, the accuracy and possibly the stability of the linearized difference equations can be affected if the step size Δx is too large for a prescribed Δy. These difficulties can be circumvented with multistep iterative techniques. In this way, the nonlinear finite-difference equations are more closely approximated and the accuracy of the calculations is improved.

For the leading-edge solutions discussed herein, iteration is essential if stable solutions are to be obtained with larger values of Δx; moreover, iteration is most likely needed with smaller Δx values if highly accurate solutions are desired. With unsteady Navier–Stokes calculations, iteration would be required to accurately describe the transient states.

Typical results of the iteration procedure are given in Table I, where an implicit Crank–Nicolson scheme was prescribed for the axisymmetric flow over a cone at zero incidence. Similar results have been obtained with an $I + 1$ centered implicit method and with other two-dimensional geometries [5]. The calculations are initiated at the leading edge and progress downstream in x to $\bar{V} = 0.08$. $\bar{V}$ is the rarefaction parameter defined in terms of the Mach number M_∞ and Reynolds number $\mathrm{Re}_\infty = U_\infty x/\nu$; $\bar{V} = \sqrt{c}M_\infty/\sqrt{(\mathrm{Re}_\infty)}$. C_H is the heat transfer coefficient defined by $C_H = [kT_y + \rho\nu u u_y]_{y=0}/\rho_\infty U_\infty c_p(T_{0_\infty} - T_w)$. k is the thermal conductivity, c_p is the specific heat at constant pressure, T the temperature, and ρ the density.

For the larger streamwise increments, $\Delta x > 0.005$, with a Taylor series linearization to $O(\Delta x^2)$, the calculations become unstable for $\bar{V} < 0.4$. With a single iteration, the instability is eliminated and the solutions are reasonably accurate. Further iteration provides increased accuracy for the flow properties and derivatives. Surface properties, shock conditions and even the small normal velocity near the surface exhibit the same tendency toward stability and accuracy. For the smallest value of Δx depicted, $\Delta x = 0.005$, the linearized calculation is stable but inaccurate. Singificant improvement is observed with a single iteration. The number of iterations required to achieve stability or high levels of accuracy is increased with linear replacement (3a) for the initial linearization. In Section V the effect of iteration as it relates to consistency of the predictor-corrector finite-difference equations is described with a simple model Burgers' equation, and in Section VI, the need for iteration in three-dimensional leading-edge calculations is discussed.

The final portion of this section is concerned with the procedure for solving the linearized difference equations. In view of the coupling associated with this semi-implicit formulation, a large number of algebraic equations must be solved simultaneously. This inversion process can become extremely time consuming as large numbers of grid points must be considered to achieve desired accuracy.

With the formulas (2), the linearized implicit difference equations of Section VI are of the general quasi-two-dimensional form

$$B_1(J)\, A_{I+1,J+1,K} + B_2(J)\, A_{I+1,J,K} + B_3(J)\, A_{I+1,J-1,K} = C_1(J), \tag{4}$$

where

$$A = \begin{pmatrix} u \\ T \\ v \\ \rho \end{pmatrix};$$

$B_K(J)$ is a square matrix and $C_m(J)$ is a column vector, the components of which are functions of conditions at stations I and $I - 1$, or $I + 1$ when evaluated with known conditions from the previous iteration. The system (4) is solved with a technique discussed by Richtmyer [13][2] and first introduced by Flugge–Lotz and Blottner [14] for boundary layer calculations. This method has proven most successful for two- and three-dimensional leading-edge numerical studies, with the latter treated by quasi-two-dimensional iterative methods [5]. The object of this algorithm is to reduce the three-point difference Eqs. (4) to two-point Eqs. (5) with appropriate use of the boundary conditions.

$$A_{I+1,J,K} = B_4(J)\, A_{I+1,J+1,K} + C_2(J). \tag{5}$$

With the boundary conditions at the surface, it is possible to substitute (5) into (4) and determine the components of $B_4(J)$ and $C_2(J)$. Then, starting with the outer boundary condition, at a given streamwise station $I + 1$, from (5), it is possible to progress inward the surface and evaluate $A_{I+1,J,K}$. If the process is reversed so that the outer boundary conditions specify $B_4(J)$ and $C_2(J)$, the calculation moves outward from the surface, but the final results are unchanged.

The advantage of this method of integration is the speed of calculation when large numbers of grid points are specified. With fifty (50) mesh points and four variables, or 200 matrix points, this method, when applied to leading-edge equations, is five times faster than the IBM GELB matrix-inversion subroutine. As the number of mesh points increases, the time differential widens.

[2] The authors would like to thank the reviewer who noted that this algorithm is also contained in the book "The Theory of Difference Games" by Godunov and Ryabenki.

IV. Iteration and Stability

The discussion of this Section will only be concerned with interior point stability. The procedures for handling boundary conditions can, in certain instances, alter the results obtained herein.

For the differential Eq. (1) with c, d, Re assumed constant, inserting the finite-difference formulas (2), centered at $I + 1$, leads to the following linear algebraic equation:

$$u^{m+1}_{I+1,J,K} = u_{I,J,K} - \kappa_1(u^{m+1}_{I+1,J+1,K} - u^{m+1}_{I+1,J-1,K}) - \kappa_2(u^{m}_{I+1,J,K+1} - u^{m}_{I+1,J,K-1}) + \beta_1(u^{m+1}_{I+1,J+1,K} + u^{m+1}_{I+1,J-1,K} - 2u^{m+1}_{I+1,J,K}) + \beta_2(u^{m}_{I+1,J,K+1} + u^{m}_{I+1,J,K-1} - 2u^{m+1}_{I+1,J,K}), \tag{6}$$

where

$$\kappa_1 = c\Delta x/2\Delta y, \quad \kappa_2 = d\Delta x/2\Delta z, \quad \beta_1 = \mathrm{Re}^{-1}\,\Delta x/\Delta y^2 > 0, \quad \beta_2 = \mathrm{Re}^{-1}\,\Delta x/\Delta z^2 > 0,$$

and m is the iteration number. Variables with subscript zero may be replaced with (3a) or (3b). In view of the linear nature of the differential equations, the following results must be used cautiously for nonlinear calculations [14].

If $u_{I,J,K} = \xi^I \exp(inJ\Delta y + ilK\Delta z)$, then a necessary and sufficient condition for the stability of the finite-difference Eq. (6) (see Ref. [13]) requires that the amplification factor ξ be such that

$$|\,\xi^2\,| = \xi\bar{\xi} \leqslant \gamma < 1. \tag{7}$$

When $m = 0$ (no iteration) and with linear replacement (3a) the amplification factor takes the form

$$\xi = (1 + 2\beta_2 \cos l\Delta z - 2i\kappa_2 \sin l\Delta z)/(1 + 2\beta_1(1 - \cos n\Delta y) + 2\beta_2 + 2i\kappa_1 \sin n\Delta y),$$

whereby the inequality (7) becomes

$$(\beta_2{}^2 - \kappa_2{}^2)\sin^2 l\Delta z + \beta_2(1 - \cos l\Delta z) + \beta_1{}^2(1 - \cos n\Delta y)^2 + \beta_1(1 - \cos n\Delta y) + 2\beta_1\beta_2(1 - \cos n\Delta y) + \kappa_2{}^2 \sin^2 n\Delta y \geqslant 0. \tag{8a}$$

When $\beta_2{}^2 \geqslant \kappa_2{}^2$, or $\mathrm{Re}_z = |\,d\,|\,\Delta z\,\mathrm{Re} = |\,w\,|\,\Delta z/\nu \leqslant 2$, the condition (8a) is automatically satisfied for all Δx. The cross-flow Reynolds number is small and viscous effects dominate.

If $\beta_2^2 < \kappa_2^2$ or $\mathrm{Re}_z > 2$, (8a) is satisfied only with

$$\Delta x \leqslant (\Delta z^2/2\nu)[(\mathrm{Re}_z/2)^2 - 1]^{-1}. \tag{8b}$$

When $\mathrm{Re}_z \to \infty$, lateral diffusion is neglected and the system becomes unstable. The stability condition (8b) is independent of Δy since the equations are implicit in the y-direction. Therefore, in order to assess the effect of iteration, we will neglect the y or implicit dependence and consider Eq. (1) with $\partial/\partial y \equiv 0$.

Without iteration, the stability condition for the two-dimensional modified explicit equations with $\kappa_1 = \beta_1 = 0$ is identically (8b). With one iteration the finite-difference equations become

1st step:

$$\bar{u}_{I+1,K} = u_{I,K} - \kappa_2(u_{I,K+1} - u_{I,K-1}) + \beta_2(u_{I,K+1} + u_{I,K-1} - 2\bar{u}_{I+1,K});$$

2nd step:

$$\tilde{u}_{I+1,K} = u_{I,K} - \kappa_2(\bar{u}_{I+1,K+1} - \bar{u}_{I+1,K-1}) + \beta_2(\bar{u}_{I+1,K+1} + \bar{u}_{I+1,K-1} - 2\tilde{u}_{I+1,K}).$$

Therefore,

$$\xi = (1 + 2\beta)^{-2}[1 + 2\beta + 2\beta\cos\theta - 2i\kappa\sin\theta + (2\beta\cos\theta - 2i\kappa\sin\theta)^2],$$

where $\beta = \beta_2$, $\kappa = \kappa_2$, $\theta = l\Delta z$. The stability condition becomes

$$\begin{aligned}\xi\bar{\xi} = (1 + 2\beta)^{-4}[&1 + 4\beta(1 + \cos\theta) + 4\beta^2(3\cos^2\theta + 2\cos\theta + 1) - 4\kappa^2\sin^2\theta \\ &+ 16\beta^3\cos^2\theta(1 + \cos\theta) - 16\beta\kappa^2\sin^2\theta(1 - \cos\theta) \\ &+ 16(\beta^2\cos^2\theta + \kappa^2\sin^2\theta)^2] \leqslant 1.\end{aligned} \tag{9a}$$

As was the case without iteration, when $\beta^2 \geqslant \kappa^2$ or $\mathrm{Re}_z \leqslant 2$, the system is stable. For $\mathrm{Re}_z > 2$, (8b) is replaced with an improved condition independent of Re_z,

$$\Delta x \leqslant \Delta z/|\,d\,|. \tag{9b}$$

(See Ref. [13], p. 291.) It is shown in [5] that any additional iteration will have only a minimal effect on altering the stability condition (9b). When Taylor series to $O(\Delta x^2)$ is used to linearize the equation, the system is stable without iteration but condition (9b) is reduced by a factor one-half (see [5, 11]).

In view of the modified stability results (8b) or (9b), it can be inferred that for three-dimensional predictor-corrector calculations, with the surface normal or y-direction treated implicitly, condition (9b) is the appropriate stability criterion with one or more iterations.

V. Iteration and Consistency

Consistency of the difference equations with the specified differential equations, as Δx, Δy, $\Delta z \to 0$, is necessary if meaningful numerical solutions are to be obtained. With certain finite-difference formulations, if the limiting value of $(\Delta x)^k/(\Delta z)^p$, as Δx, $\Delta z \to 0$ is prescribed improperly, stable and converged results can be obtained, but may be consistent with the analytic solution of a different differential equation than that being considered. A well-known example of this inconsistency occurs with the DuFort–Frankel method when $\Delta x/\Delta z$ is held constant [13].

[redacted]

corrector formulation presented in this paper. As in Section IV only linear differential equations are discussed and it should be emphasized that the results obtained herein cannot always be carried over to nonlinear situations.

Consider the differential Eq. (1) with $\partial/\partial y = 0$, $\epsilon = 1$; $u_x + du_z = \mathrm{Re}^{-1} u_{zz}$; Re^{-1} and d are assumed here to be constants. With a modified multistep formulation, Eqs. (2), the difference equations centered at $(I + \frac{1}{2})$ are:

0 *iteration–linear replacement,* (3a):

$$\bar{u}_{I+1,K} = u_{I,K} - \kappa(u_{I,K+1} - u_{I,K-1}) + \beta(u_{I,K+1} + u_{I,K-1} - u_{I,K} - \bar{u}_{I+1,K}); \tag{10a}$$

0 *iteration–Taylor series* $O(\Delta x^2)$, (3b):

$$\bar{u}_{I+1,K} = u_{I,K} - \tfrac{1}{2}\kappa(3u_{I,K+1} - u_{I-1,K+1} - 3u_{I,K-1} + u_{I-1,K-1}) + \tfrac{1}{2}\beta(3u_{I,K+1} - u_{I-1,K+1} + 3u_{I,K-1} - u_{I-1,K-1} - 2\bar{u}_{I+1,K} - 2u_{I,K}); \tag{10b}$$

1 *iteration*:

$$\tilde{u}_{I+1,K} = u_{I,K} - \tfrac{1}{2}\kappa(\bar{u}_{I+1,K+1} - \bar{u}_{I+1,K-1} + u_{I,K+1} - u_{I,K-1}) + \tfrac{1}{2}\beta(\bar{u}_{I+1,K+1} + \bar{u}_{I+1,K-1} + u_{I,K+1} + u_{I,K-1} - 2u_{I,K} - 2\tilde{u}_{I+1,K}); \tag{10c}$$

2 *iterations*:

$$\hat{u}_{I+1,K} = u_{I,K} - \tfrac{1}{2}\kappa(\tilde{u}_{I+1,K+1} - \tilde{u}_{I+1,K-1} + u_{I,K+1} - u_{I,K-1}) + \tfrac{1}{2}\beta(\tilde{u}_{I+1,K+1} + \tilde{u}_{I+1,K-1} + u_{I,K+1} + u_{I,K-1} - 2u_{I,K} - 2\hat{u}_{I+1,K}). \tag{10d}$$

Rewriting the difference equations, as in a one-step method, and replacing the difference quotients by their differential expressions, evaluated at the point $(I + \frac{1}{2}, K)$, for $\Delta x \to 0$, $\Delta z \to 0$, β fixed, we obtain

(a) *linear replacement*:

0 *iteration*:

$$u_x = (-du_z + \mathrm{Re}^{-1} u_{zz})\,\alpha_0 - \alpha_0(\Delta x/2)\,u_{xx} + O(\Delta x^2, \Delta z^2); \tag{11a}$$

1 *iteration*:

$$u_x = (-du_z + \mathrm{Re}^{-1} u_{zz})\,\alpha_1 - \alpha_1(\Delta x/2)\,u_{xx} + [d^2\Delta x/2(1+\beta)^2]\,u_{zz} + O(\Delta x^2, \Delta z^2), \quad \text{(Cheng [12])}; \tag{11b}$$

2 *iterations*:

$$u_x = (-du_z + \mathrm{Re}^{-1} u_{zz})\,\alpha_2 - \alpha_2(\Delta x/2)\,u_{xx} + [d^2\Delta x/2(1+\beta)^3]\,u_{zz} + O(\Delta x^2, \Delta z^2). \tag{11c}$$

(b) *Taylor series* $O(\Delta x^2)$:

0 *iteration*:

$$u_x = (-du_z + \mathrm{Re}^{-1} u_{zz}) - \beta\Delta x u_{xx} + O(\Delta x^2, \Delta z^2), \quad \text{(Crocco [11])}; \tag{12a}$$

1 *iteration*:

$$u_x = (-du_z + \mathrm{Re}^{-1} u_{zz}) - [\Delta x/2(1+2\beta)][u_{xx} - d^2 u_{zz}] + O(\Delta x^2, \Delta z^2), \tag{12b}$$

where $\beta = \mathrm{Re}^{-1}\,\Delta x/\Delta z^2$, $\kappa = d\Delta x/2\Delta z$ and $\alpha_n = 1 - [\beta/(1+\beta)]^{n+1}$. When the difference equations are centered at $I + 1$, similar results are obtained but with $\alpha_n = 1 - [2\beta/(1+2\beta)]^{n+1}$ (see Ref. [5]).

TABLE II

Effect of Iteration on Consistency with Linear Replacement

β	α_0	α_1	α_2	α_3	α_4
0	1	1	1	1	1
0.25	0.800	0.960	0.992	0.998	0.999
0.50	0.667	0.889	0.963	0.988	0.996
1	0.500	0.750	0.875	0.938	0.969
2	0.333	0.556	0.705	0.802	0.868

Terms of order Δx have been retained in (11) and (12) so that we can assess the effect of iteration when Δx is small but nonzero. From (11) and (12) we can conclude that consistency is achieved as $\Delta x \to 0$ *for all finite* β with Taylor-series replacement, but only for $\beta \to 0$ with a simple linear replacement.

From a practical point of view, consistency in (a) can be achieved for all finite β with sufficient iteration, since for $\beta > 0$, $\lim_{n\to\infty} \alpha_n \to 1$. Table II lists α_n for selected β values.

It is also significant that iteration reduces the magnitude of the error terms as given in (11) and (12).

For actual calculations where Δx is small but finite, one would expect that with Taylor-series replacement, consistency to any order of iteration can be achieved with somewhat larger values of β, as the error in (12) is smaller by Δx than that of (11) (see Fig. 3). Even larger β values are permissible with a reduced number of iterations when the $I - 2$ plane is added to the expansion and the error terms in (12) are order $\beta\Delta x^2$. However, storage requirements are increased.

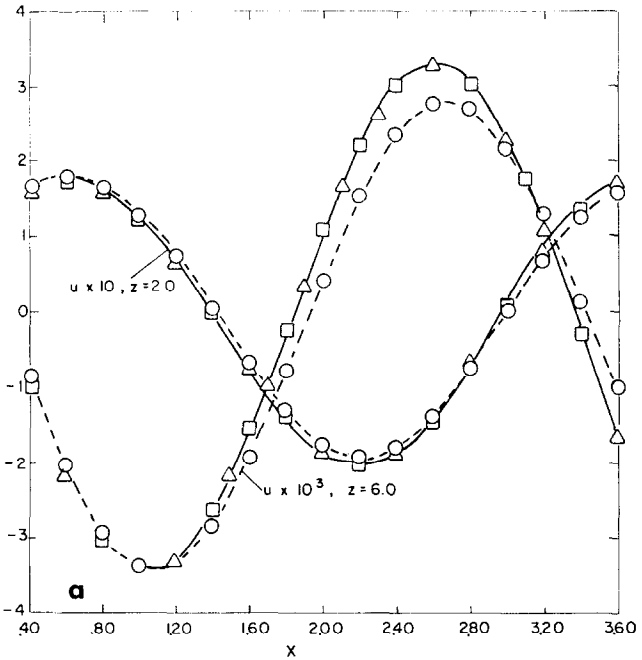

ΔX=0.01, Δz=0.2, $\beta = \Delta X/\Delta z^2 = 0.25$
○ MODIFIED EXPLICIT SCHEME (1 ITERATION WITH LINEAR REPLACEMENT)
□ FULLY IMPLICIT METHOD
△ MODIFIED EXPLICIT SCHEME (2 ITERATIONS WITH TAYLOR SERIES EXPANSION $O(\Delta x^2)$)

FIG. 3. (a) Modified explicit solutions-effect of iteration;

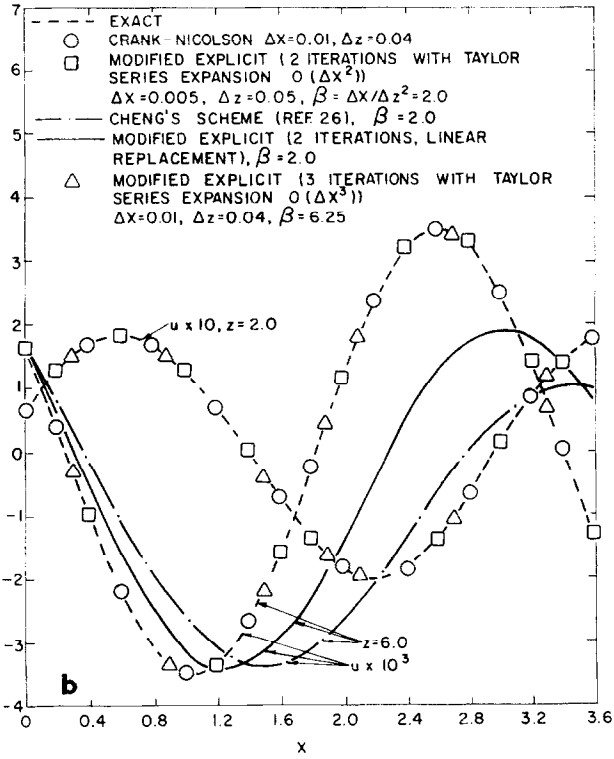

Fig. 3. (b) modified explicit solutions-effect of iteration.

With $\beta \leqslant 6$ and a Taylor-series linearization of $O(\Delta x^2)$, it is found that three iterations are required for the three-dimensional leading-edge predictor-corrector calculations; whereas, except for extreme cases, only one is necessary for the two-dimensional implicit solutions (see Table I). For even larger values of β, but within the limitations of the stability condition (9b), additional iteration is needed if consistent finite-difference solutions are to be obtained: With implicit methods, successive approximation is necessitated solely by linearization. With approximate derivative representations, such as (2e), consistency of the difference equations with the differential equations, for larger Δx values, is dependent on sufficient additional iteration.

The need for increased iteration with the modified explicit formulas (2e) is shown by consideration of Eq. (1) with $\partial/\partial y \equiv 0$, Re $= 1$, $\epsilon = 1$ and $d = u$ (Burgers' equation). As shown by Cheng [12], the exact solution of this equation is

$$u = [\cos(z - 2x) + \sin(z - 2x)]/[e^z + \tfrac{1}{2}\cos(z - 2x)].$$

Calculations have been made with an $I + 1$ centered implicit model (fully implicit), Crank–Nicolson model, two-step (one iteration) modified explicit formulation with linear replacement, three-step (two iterations) modified explicit model with linear replacement, a three-step modified explicit model with a Taylor-series expansion of $O(\Delta x^2)$ for the initial linearized values (this is superior to a three-iteration approach with linear replacement), and Taylor-series linearization of $O(\Delta x^3)$. Results are shown on Fig. 3. It is clear that at least two and most likely three iterations are required if the modified solution is to compare favorably with an exact implicit formulation without iteration. With sufficient iteration, the agreement is excellent and the consistency of the modified approach is confirmed. It is significant that for all the calculations depicted ($\beta < 6.25$), the stability condition (9b) is satisfied, yet more than one iteration is required if consistent solutions are to be obtained. With only one iteration and $\beta = 2$, the numerical solution differs significantly from the exact result. If one is to accurately represent transient motion ($x \to t$) with this modified formulation, multiple iteration is a necessity; in addition, the use of a Taylor series expansion of $O(\Delta x^2)$ in the first step, for the linearized terms, reduces the number of required iterations, and, therefore, leads to reduced computational times without increasing storage requirements. These results support the consistency analysis presented in the beginning of this Section.

For the three-dimensional multistep calculations presented in Section VI, only the lateral derivatives are specified with the modified explicit expressions, with the surface normal direction treated implicitly, [see Eqs. (2)]. The relevant value of β is $\nu\Delta x/u\Delta z^2$. For the calculations presented in Section VI, $\beta \leqslant 2$ with linear replacement and $\beta \leqslant 6$ with Taylor series replacement of $O(\Delta x^2)$. For the explicit three-dimensional calculations $\beta < 0.05$. The consistency of the semi-implicit method shown is demonstrated on Figs. 5 and 6.

VI. Right-Angle Corner

The predictor-corrector method presented herein has been used to examine the hypersonic viscous flow along a right-angle corner. This geometry has been examined previously by explicit methods [6], but only in the region $\bar{V} > 0.25$. With the semi-implicit iterative method, computer times have been substantially reduced and the calculations for the same stream conditions have been extended to $\bar{V} = 0.17$, where imbedded shock formation is predicted. In addition, solutions are obtained for two other flow conditions for which there is recent experimental data [15, 16].

The three-dimensional single-layer equations that are used to calculate leading-edge flow fields have been derived in Ref. [4] and are discussed further in Refs. [5, 6].

The governing system of equations is as follows:

$$
\begin{aligned}
(\rho u)_x + (\rho v)_y + (\rho w)_z &= 0,\\
\rho u u_x + \rho v u_y + \rho w u_z &= -p_x + (\mu u_y)_y + (\mu u_z)_z\,,\\
\rho u v_x + \rho v v_y + \rho w v_z &= -p_y + (4/3)(\mu v_y)_y + (\mu u_y)_x\\
&\quad + (\mu w_y)_z + (\mu v_z)_z - (2/3)[(\mu u_x)_y + (\mu w_z)_y],\\
\rho u w_x + \rho v w_y + \rho w w_z &= -p_z + (4/3)(\mu w_z)_z + (\mu u_z)_x\\
&\quad + (\mu v_z)_y + (\mu w_y)_y - (2/3)[(\mu u_x)_z + (\mu v_y)_z], \qquad (13)\\
\rho u T_x + \rho v T_y + \rho w T_z &= -(\gamma - 1)\,p(u_x + v_y + w_z) + (\gamma/\sigma)[(\mu T_y)_y\\
&\quad + (\mu T_z)_z] + \gamma(\gamma - 1)\,M_\infty{}^2\mu[u_y{}^2 + u_z{}^2]\\
&\quad + (4/3)\,\mu(\gamma - 1)[v_y{}^2 + w_z{}^2 - v_y w_z]\\
&\quad + \mu(\gamma - 1)(w_y + v_z)^2,\\
p &= \rho T.
\end{aligned}
$$

The Sutherland viscosity law with a suitable correction for $\bar{T} < 180°\mathrm{R}$ is used throughout. All quantities are nondimensional: $\nu = \bar{\nu}/\bar{\nu}_\infty M_\infty$; $x = \bar{x}/\bar{\mathscr{L}}$; $y = \bar{y}/\delta\bar{\mathscr{L}}$; $\bar{\mathscr{L}} = \gamma_\infty M_\infty{}^3\bar{\nu}_\infty/\bar{u}_\infty$; $\delta = (\gamma^{1/2}M_\infty)^{-1}$; $\gamma_\infty = 1.4$; $\sigma = 0.75$; all other properties are nondimensionalized with their free-stream values. Bars denote dimensional properties.

Slip boundary conditions are enforced at the surface, to allow for low-density effects. Symmetry conditions are prescribed across the diagonal. Along the surface, $y = 0$, $z > 0$:

$$
\begin{gathered}
v = 0; \qquad T = T_w + [2\gamma/(\gamma + 1)](\lambda/\sigma)\,T_y\,, \qquad u = \lambda u_y\,,\\
w = \lambda[w_y + 3(8\pi T)^{-1/2}\,T_z]; \qquad \lambda = 1.26\nu/T^{1/2}.
\end{gathered} \qquad (14)
$$

As discussed in great detail in Refs. [1–4], for the leading-edge equations, the downstream influence of rather arbitrary initial conditions decays rapidly and [illegible] $\bar{V} = \sqrt{1/M_\infty{}^2} \leqslant 0.4$. In

theory approach to the leading-edge flow, the present theory should then only be applicable to the range $\bar{V} \leqslant 0.5$.

Initial conditions are prescribed to satisfy the boundary conditions (14); in addition, the heat-transfer coefficient and wall density at the leading-edge surface mesh point are set equal to their respective free molecular values, and the surface pressure is anywhere from one to three times its free molecular value. Apart from satisfying a mass flux condition, all other initial values are arbitrary. These conditions were chosen as they closely approximate most of the available leading-

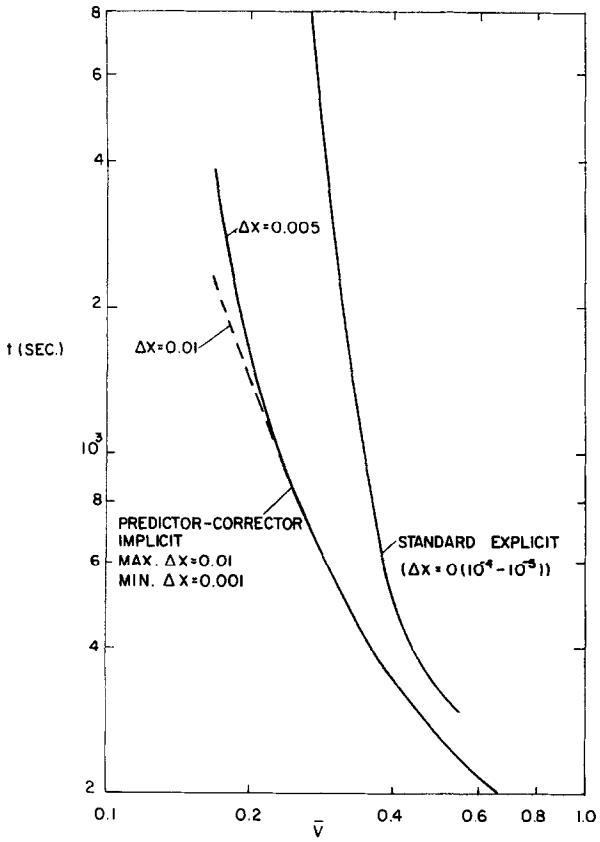

FIG. 4. Computer times-three-dimensional corner.

edge surface data. Agreement with this data is then good for $\bar{V} > 0.5$, even though the initial values are not exact and the continuum theory is questionable in this region, see [1, 3, 4].

On Fig. 4, a comparison of the computer times for the implicit and explicit solutions is depicted. For these calculations, $M_\infty = 11.2$, $T_w/T_0 = 0.30$, $\Delta y = 0.08$, $\Delta z = 0.08$ near the corner, with Δz increasing to 0.64 in the asymptotic two-dimensional flow. The maximum lateral grid point is $K = K_{\text{Max}}$ and defined when

$$| A_{I+1,J,K_{\text{Max}}} - A_{I+1,J,K_{\text{Max}}-3} | < 10^{-4}; \qquad A = u, T, w.$$

The iteration cycle proceeds from right to left (toward the corner) in the lateral direction; symmetry at the 45° line is maintained with $u_{I+1,J+1,K} = u_{I+1,J,K+1}$ and $w_{I+1,J+1,K} = v_{I+1,J,K+1}$. To reach a location $\bar{V} = 0.25$ the explicit method requires approximately 170 min on a CDC 6600 computer; the implicit solution was obtained

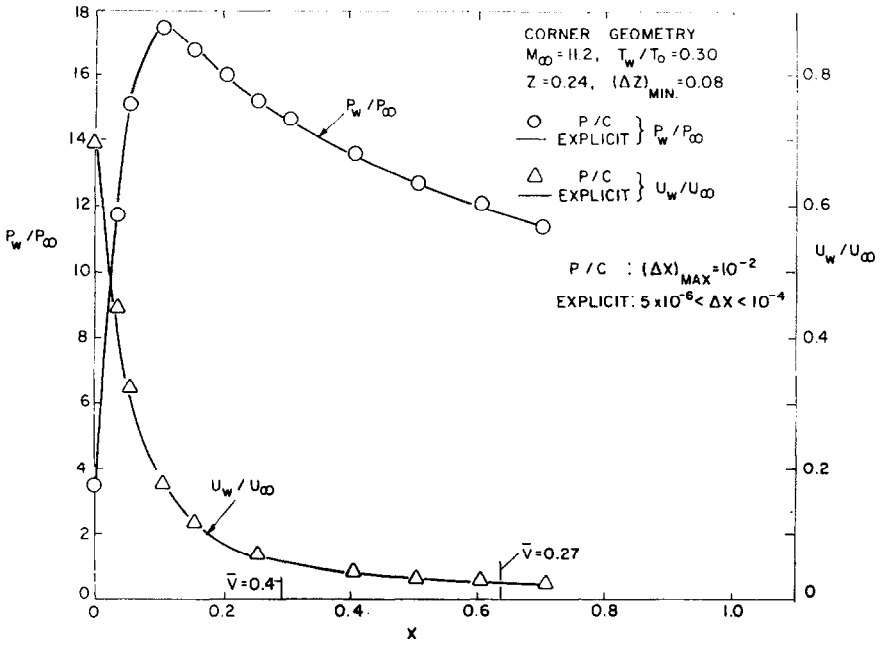

FIG. 5. Predictor-corrector vs explicit solutions: surface values in stream direction.

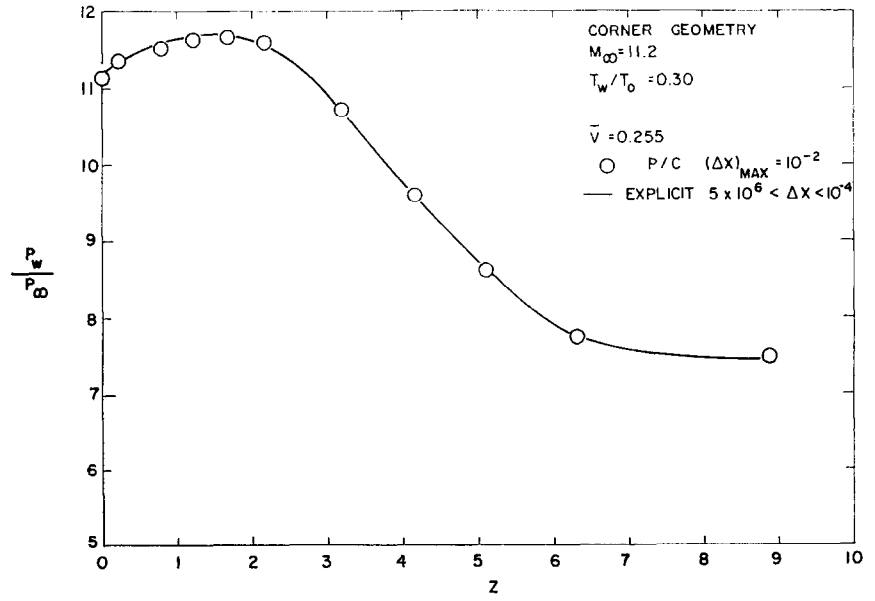

FIG. 6. Comparison between explicit and predictor-corrector (P/C) solutions.

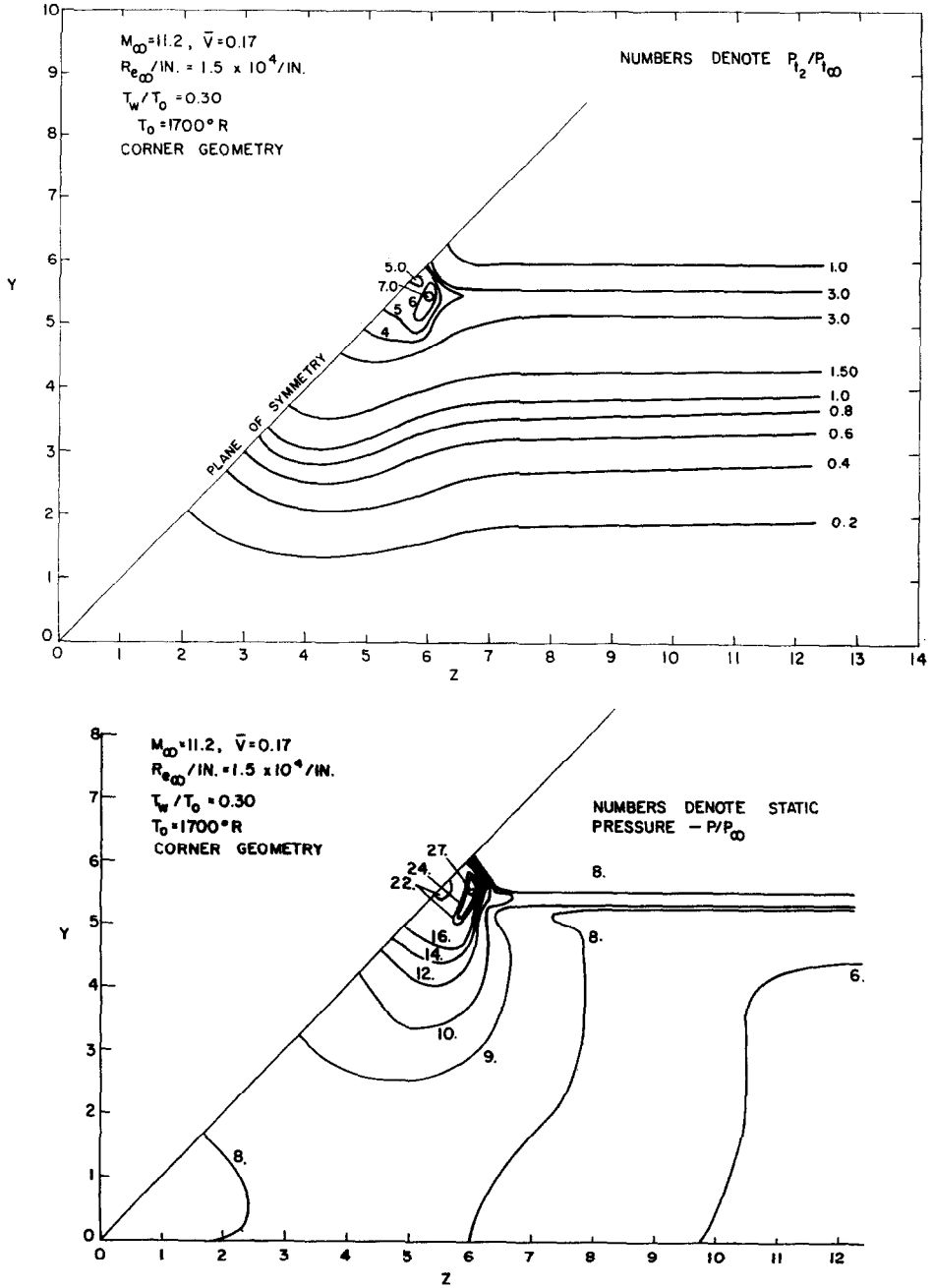

FIG. 7. (a) Theoretical Pitot pressure contours in corner region at $\bar{V} = 0.17$; (b) theoretical isobars in corner region at $\bar{V} = 0.17$.

in approximately thirteen (13) min. Four iterations were prescribed initially for each point. Three appear to be adequate as you progress further downstream, $\bar{V} < 0.30$.

For this corner geometry the calculation times, even with implicit methods, become excessive for solutions very far downstream. As the extent of the three-dimensional interference region increases, the number of required mesh points grows very rapidly, even with symmetry conditions applied along the centerline. For a cone at incidence, with the use of a cylindrical-body fixed coordinate system, the computer times are considerably less than for the corner geometry. $\bar{V} = 0.1$ is reached in approximately twenty (20) min.[3]

Figures 5 and 6 show a comparison of implicit and explicit solutions along the surface, in the stream direction for $\bar{V} > 0.255$, and in the lateral direction at $\bar{V} = 0.255$. The agreement is excellent. This is true for the shock layer profiles as well, and indicates that the handling of the lateral derivatives by this predictor-corrector method leads to a finite-difference system that is consistent with the explicit method, and therefore, the differential equations. When the number of

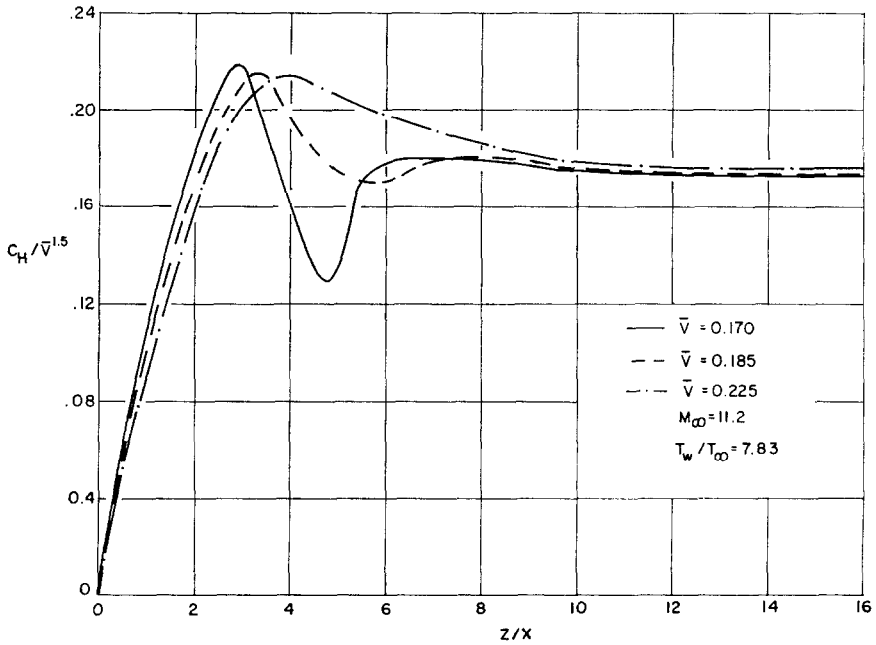

FIG. 8. Heat-transfer distribution for a corner geometry—$M_\infty = 11.2$.

[3] At this location the calculation has progressed 200 steps in the x or marching direction. The leading-edge solutions to $\bar{V} = 0.1$ have been obtained and comparisons with explicit calculations and some pressure data are excellent. The calculation is being extended downstream with a modified viscous-interaction analysis.

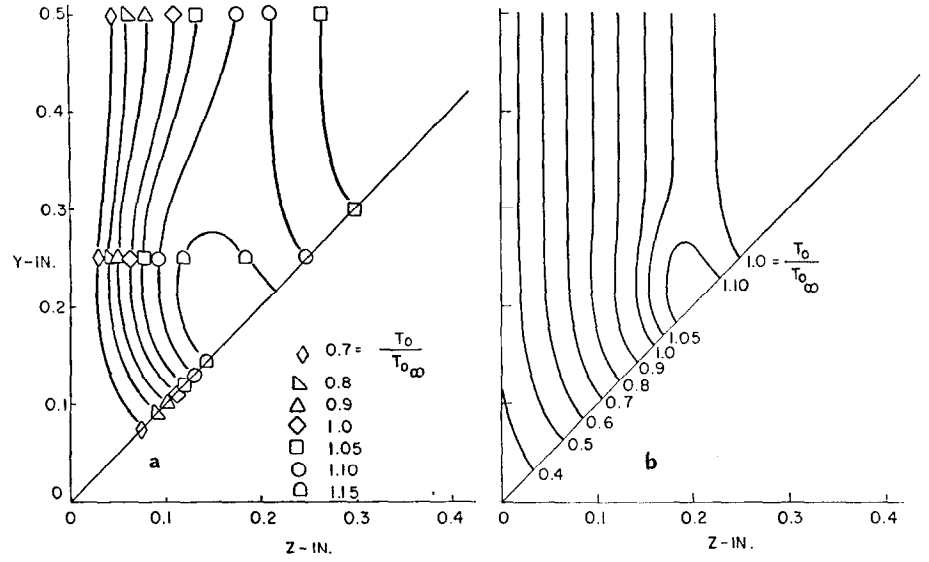

FIG. 9. Stagnation temperature contours ($\bar{V} = 0.39$). (a) Experimental data, Ref. [15]; (b) present theory.

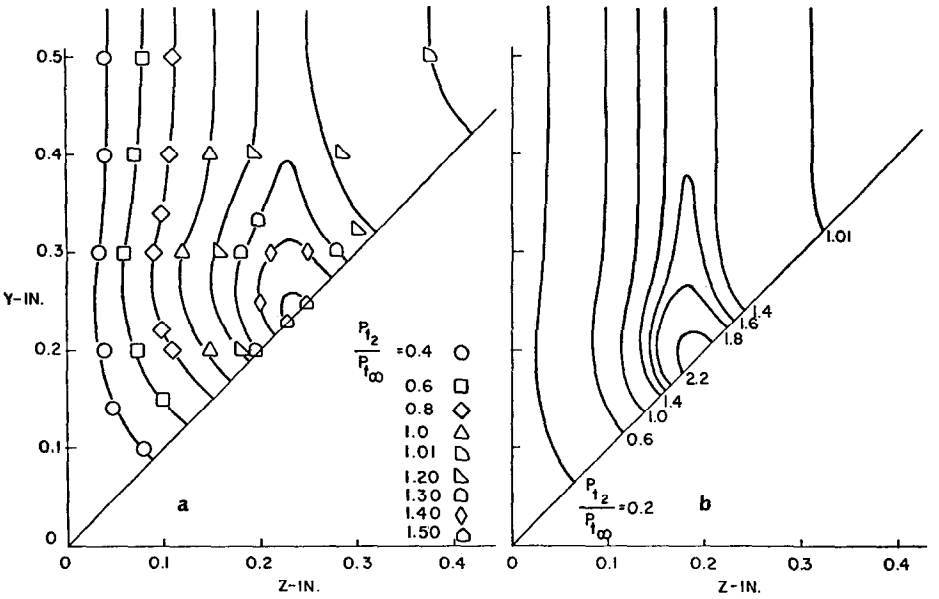

FIG. 10. Pitot pressure contours ($\bar{V} = 0.39$). (a) Experimental data, Ref. [15]; (b) present theory.

iterations is decreased, the predictor-corrector and explicit solutions are no longer in good agreement. An inconsistency similar to that occurring with Burgers' equation arises, see Section V.

For the implicit calculations, step sizes in the marching or x-direction vary from a minimum of 10^{-3} near the leading edge to a maximum of 10^{-2}. As the calculation progresses downstream, it is possible to increase Δx significantly and insure acceptable accuracy within the postulated stability requirements. For the explicit calculations $\Delta x < 10^{-4}$. It has been shown by Rubin and Lin [5] that decreasing Δy, Δz has little or no effect on the solutions, except in the shock structure for strong shock waves where the validity of the Navier–Stokes model is questionable.

Figure 7 depicts pressure contours at $\bar{V} = 0.17$; the formation of an internal imbedded shock wave is predicted. These results can be compared with corner solutions at a location further upstream where no internal waves are apparent, or experimental values much further downstream where shock patterns are now

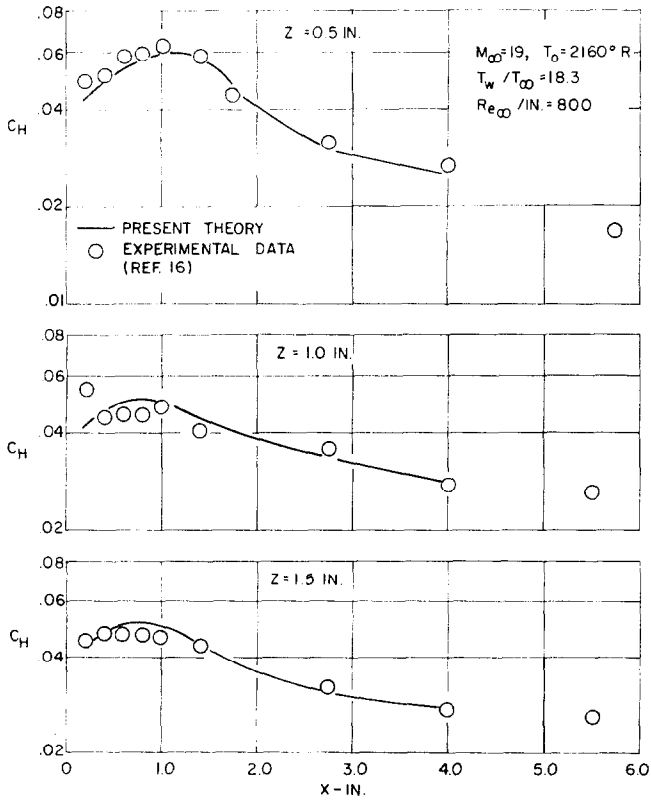

FIG. 11. Streamwise heat-transfer history—$M_\infty = 19$.

quite distinct, see Ref. [6]. The surface heat-transfer distribution at several streamwise locations is shown on Fig. 8. Very close to the leading edge an overshoot in the heat transfer appears near the corner intersection line. Further downstream this overshoot is followed by a region where C_H falls below its asymptotic two-dimensional value. These results confirm similar behavior found in experimental data at streamwise locations near [16] and far [6, 17] from the leading edge.

Comparisons with recent data for the leading edge corner region are shown in Figs. 9–11. Cresci and Schmidt [15] have obtained impact pressure and recovery temperature distributions, Figs. 9, 10, but no surface data. The experimental pressure data has not been corrected for local Mach-number or Reynolds-number

several distances from the corner intersection line, Fig. 11. The agreement is very good and well within the experimental error and accuracy of the theoretical analysis.

VII. Summary and Conclusions

A predictor-corrector semi-implicit finite-difference method has been critically examined in order to test its effectiveness in solving three-dimensional viscous-flow problems. Specific application has been made to hypersonic leading-edge flows. The method is applicable to the unsteady two-dimensional Navier–Stokes equations and three-dimensional boundary-layer equations as well. A model equation, representative of three-dimensional viscous flow equations, has been analyzed.

From leading-edge solutions and analysis of the model equation it was found that:

(1) One iteration is generally sufficient to recover acceptable accuracy when nonlinear difference equations are linearized with Taylor-series expansions correct to $O(\Delta x^2)$.

(2) One iteration is sufficient to significantly improve the stability of the system. Since this method is implicit in the surface normal or y-direction, stability conditions depend solely on the lateral grid dimension. Further iteration does little to modify the stability criteria.

(3) Several iterations are required to achieve consistency of the difference equations with the differential equations. The better the initial linearization the fewer the iterations that are needed with a given streamwise increment Δx. Taylor-series linearization to $O(\Delta x^2)$ is significantly better than linear replacement of $O(\Delta x)$. As the grid spacing Δx increases, but remains well within the stability limitation, additional iteration becomes necessary.

(4) Semi-implicit solutions for a corner geometry are in excellent agreement with explicit results obtained with Δx two orders-of-magnitude smaller and with calculation times more than an order-of-magnitude greater.

(5) Comparisons with available experimental data for the corner geometry are very good.

Considerations for the flow over a cone at incidence are nearing completion and preliminary work on unsteady Navier–Stokes solutions is in progress.

REFERENCES

1. S. RUDMAN AND S. G. RUBIN, *AIAA J.* **6** (1968), 1883.
2. H. K. CHENG, Y. S. CHEN, R. MOBLEY, AND C. HUBER, "Rarefied Gas Dynamics" (L. Trilling and H. Y. Wachman, Eds.), Vol. 1, p. 451, Academic Press, New York, 1969.
3. S. G. RUBIN AND T. C. LIN, "Paper presented at 7th International Symposium on Rarefied Gas Dynamics," Pisa, Italy, July 1970 (Proceedings to appear 1971).
4. S. G. RUBIN, T. C. LIN, M. PIERUCCI, AND S. RUDMAN, *AIAA J.* **7** (1969), 1744.
5. S. G. RUBIN AND T. C. LIN, PIBAL Report No. 71-8, Polytechnic Institute of Brooklyn, April, 1971.
6. R. J. CRESCI, S. G. RUBIN, C. NARDO, AND T. LIN, *AIAA J.* **7** (1969), 2241.
7. C. T. NARDO AND R. J. CRESCI, AIAA Paper No. 70-784, presented at AIAA 3rd Fluid and Plasma Dynamics Conference, June 1970.
8. D. W. PEACEMAN AND H. H. RACHFORD, *J. Soc. Ind. Appl. Math.* **3** (1955), 28.
9. E. KRAUSE, *AIAA J.* **7** (1969), 575.
10. G. W. EVANS, R. BROUSSEAU, AND R. KIERSTEAD, *J. Math. Phys.* **34** (1955), 267.
11. L. CROCCO, *AIAA J.* **3** (1965), 1824.
12. S. I. CHENG, *AIAA J.* **8** (1970), 2115.
13. R. D. RICHTMYER AND K. W. MORTON, "Difference Methods for Initial Value Problems," 2nd ed., Interscience Publishers, New York, 1967.
14. I. FLÜGGE-LOTZ AND F. G. BLOTTNER, Technical Report No. TR-131, Stanford University, 1962 (See also *J. Mec.* **2** (1963), 397.)
15. R. J. CRESCI AND E. SCHMIDT, Paper presented at 7th International Symposium on Rarefied Gas Dynamics, Pisa, Italy, July 1970 (Proceedings to appear 1971).
16. H. T. NAGAMATSU, R. E. SHEER, JR., AND W. T. PETTIT, Report No. 70-C-392, General Electric Company, Schenectady, N.Y., November, 1970.
17. R. D. WATSON AND L. M. WEINSTEIN, AIAA Paper No. 70-227, presented at 8th Aerospace Sciences Meeting, New York, January, 1970.